

Quincy Teng

Structural Biology

Practical NMR Applications

Second Edition

 Springer

Structural Biology

Quincy Teng

Structural Biology

Practical NMR Applications

Second Edition

 Springer

Quincy Teng
Department of Pharmaceutical
and Biomedical Sciences
College of Pharmacy
University of Georgia
Athens, GA, USA

ISBN 978-1-4614-3963-9 ISBN 978-1-4614-3964-6 (eBook)
DOI 10.1007/978-1-4614-3964-6
Springer New York Heidelberg Dordrecht London

Library of Congress Control Number: 2012942118

© Springer Science+Business Media New York 2013

This work is subject to copyright. All rights are reserved by the Publisher, whether the whole or part of the material is concerned, specifically the rights of translation, reprinting, reuse of illustrations, recitation, broadcasting, reproduction on microfilms or in any other physical way, and transmission or information storage and retrieval, electronic adaptation, computer software, or by similar or dissimilar methodology now known or hereafter developed. Exempted from this legal reservation are brief excerpts in connection with reviews or scholarly analysis or material supplied specifically for the purpose of being entered and executed on a computer system, for exclusive use by the purchaser of the work. Duplication of this publication or parts thereof is permitted only under the provisions of the Copyright Law of the Publisher's location, in its current version, and permission for use must always be obtained from Springer. Permissions for use may be obtained through RightsLink at the Copyright Clearance Center. Violations are liable to prosecution under the respective Copyright Law.

The use of general descriptive names, registered names, trademarks, service marks, etc. in this publication does not imply, even in the absence of a specific statement, that such names are exempt from the relevant protective laws and regulations and therefore free for general use.

While the advice and information in this book are believed to be true and accurate at the date of publication, neither the authors nor the editors nor the publisher can accept any legal responsibility for any errors or omissions that may be made. The publisher makes no warranty, express or implied, with respect to the material contained herein.

Printed on acid-free paper

Springer is part of Springer Science+Business Media (www.springer.com)

Preface

The second edition of “Structural Biology: Practical NMR Applications” retains the focus of the previous edition, which is to provide readers with a systematic understanding of fundamental principles and practical aspects of NMR spectroscopy. At the beginning of each section, questions and objectives highlight key points to be learned, and homework problems are provided at the end of each chapter, except Chap. 9. One hundred multiple-choice questions with answers are provided to further aid in understanding the topics. In response to comments and suggestions from readers, and based on my own research and teaching experiences, I have made improvements and added a new chapter (Chap. 9) on metabolomics, which is an important application of NMR spectroscopy.

Over the years since NMR was first applied to solve problems in structural biology, it has undergone dramatic developments in both NMR instrument hardware and methodology. While it is established that NMR is one of the most powerful tools for understanding biological processes at the atomic level, it has become increasingly difficult for authors and instructors to make valid decisions concerning the content and level for a graduate course of NMR spectroscopy in structural biology. Because many of the details in practical NMR are not documented systematically, students entering into the field have to learn the experiments and methods through communication with other experienced students or experts. Often such a learning process is incomplete and unsystematic. This book is meant to be not only a textbook but also a handbook for those who routinely use NMR to study various biological systems. Thus, the book is organized with experimentalists in mind, whether they are instructors or students. For those who have a little or no background in NMR structural biology, it is hoped that this book will provide sufficient perspective and insight. Those who already have NMR research experience may find new information or different methods that are useful to their research.

Because understanding fundamental principles and concepts of NMR spectroscopy is essential for the application of NMR methods to research projects, the book begins with an introduction to basic NMR principles. While detailed mathematics and quantum mechanics dealing with NMR theory have been addressed in several

well-known NMR books, Chap. 1 illustrates some of the fundamental principles and concepts of NMR spectroscopy in a more descriptive and straightforward manner. Such questions as, “How is the NMR signal generated? How do nuclear spins behave during and after different radio-frequency pulses? What is the rotating frame, and why do we need it?” are addressed in Chap. 1. Next, NMR instrumentation is discussed starting with hardware components. Topics include magnetic field homogeneity and stability, signal generation and detection, probe circuits, cryogenic probes, analog-to-digital conversion, and test equipment. A typical specification for an NMR spectrometer is also included in the chapter. There is also a chapter covering NMR sample preparation, a process that is often the bottleneck for the success of the NMR project. Several routine strategies for preparing samples for macromolecules as well as complexes are dealt with in detail.

Chapter 4 discusses the practical aspects of NMR, including probe tuning, magnet shimming and locking, instrument calibrations, pulse field gradients, solvent suppression, data acquisition and processing, and homonuclear two-dimensional experiments. In Chap. 5, experiments that are routinely used in studying biological molecules are discussed. Questions to be addressed include how the experiments are setup and what kind of information we can obtain from the experiments.

The next chapter focuses on the application of NMR techniques to the study of biological molecules. The use of NMR in studying small biological molecules such as ligands, drugs, and amino acids involved in different biological pathways is covered. Then, applications in studies of macromolecules such as proteins, protein-peptide, and protein-protein complexes are discussed in Chap. 7. Chapter 8 deals with dynamics of macromolecules, important information that can be obtained uniquely by NMR methods.

Chapter 9 discusses essential principles and applications of NMR-based metabolomics. First, fundamentals of multivariate analysis are addressed in a simple and easily understood manner. The next section focuses on sample preparation, which includes detailed procedures and protocols on collecting and preparing biofluid samples, quenching cells and tissues, and extracting metabolites from cells and tissues. Practical aspects of NMR experiments routinely used in metabolomics are also discussed in detail, including experimental setup, data processing and interpretation. In the next section, a number of examples are worked out in detail to illustrate statistical analyses of NMR data and interpretation of the statistical models. Several protocols for using software packages for multivariate analysis are also provided in this section. The last four sections focus on applications of NMR-based metabolomics, including metabolomics of biofluids, cellular metabolomics, live cells, and applications to cancer research.

I would like to thank many colleagues who have used the previous edition in their teaching, and those who have contributed directly or indirectly to this book. I am particularly grateful to Dr. Jun Qin for writing sections of Chaps. 3 and 7, and for numerous discussions, and Drs. Kristen Mayer, Weidong Hu, Steve Unger, Fang Tian, John Glushka, Chalet Tan, Drew Ekman, and Timothy Collette for reviewing all or part of the text and providing corrections, valuable comments, and

encouragement. I am appreciative of the investigators and publishers who have allowed me to use their figures in this text. I am also indebted to the editors and staff at Springer Science+Business Media, especially to Editor Portia Formento, Senior Editor Andrea Macaluso, and Senior Publication Editors Patrick Carr and Felix Portnoy, who made this book happen.

Athens, GA, USA

Quincy Teng

Contents

1	Basic Principles of NMR	1
1.1	Introduction	1
1.2	Nuclear Spin in a Static Magnetic Field	2
1.2.1	Precession of Nuclear Spins in a Magnetic Field	2
1.2.2	Energy States and Population	4
1.2.3	Bulk Magnetization	5
1.3	Rotating Frame	6
1.4	Bloch Equations	11
1.5	Fourier Transformation and Its Applications in NMR	13
1.5.1	Fourier Transformation and Its Properties Useful for NMR	13
1.5.2	Excitation Bandwidth	15
1.5.3	Quadrature Detection	17
1.6	Nyquist Theorem and Digital Filters	18
1.7	Chemical Shift	20
1.8	Nuclear Coupling	26
1.8.1	Scalar Coupling	26
1.8.2	Spin Systems	29
1.8.3	Dipolar Interaction	30
1.8.4	Residual Dipolar Coupling	31
1.9	Nuclear Overhauser Effect	36
1.10	Relaxation	39
1.10.1	Correlation Time and Spectral Density Function	40
1.10.2	Spin–Lattice Relaxation	41
1.10.3	T ₂ Relaxation	44
1.11	Selection of Coherence Transfer Pathways	47

1.12	Approaches to Understanding NMR Experiments	48
1.12.1	Vector Model	48
1.12.2	Product Operator Description of Building Blocks in a Pulse Sequence	49
1.12.3	Introduction to Density Matrix	54
	Appendix A: Product Operators	59
	References	61
2	Instrumentation	65
2.1	System Overview	65
2.2	Magnet	65
2.3	Transmitter	69
2.4	Receiver	74
2.5	Probe	77
2.6	Quarter-Wavelength Cable	85
2.7	Analog/Digital Converters	87
2.8	Instrument Specifications	90
2.9	Test or Measurement Equipment	92
2.9.1	Reflection Bridge	92
2.9.2	Oscilloscope	93
2.9.3	Spectrum Analyzer	96
2.9.4	System Noise Measurement	98
	References	101
3	NMR Sample Preparation	103
3.1	Introduction	103
3.2	Expression Systems	104
3.2.1	Escherichia coli Expression Systems	104
3.2.2	Fusion Proteins in the Expression Vectors	105
3.2.3	Optimization of Protein Expression	106
3.3	Overexpression of Isotope-Labeled Proteins	107
3.4	Purification of Isotope-Labeled Proteins	108
3.5	NMR Sample Preparation	109
3.5.1	General Considerations	109
3.5.2	Preparation of Protein–Peptide Complexes	109
3.5.3	Preparation of Protein–Protein Complexes	110
3.5.4	Preparation of Alignment Media for Residual Dipolar Coupling Measurement	111
3.6	Examples of Protocols for Preparing $^{15}\text{N}/^{13}\text{C}$ Labeled Proteins . . .	113
3.6.1	Example 1: Sample Preparation of an LIM Domain Using Protease Cleavage	113
3.6.2	Example 2: Sample Preparation Using a Denaturation–Renaturation Method	114
	References	115

4 Practical Aspects	117
4.1 Tuning the Probe	118
4.2 Shimming and Locking	120
4.3 Instrument Calibrations	123
4.3.1 Calibration of Variable Temperature	123
4.3.2 Calibration of Chemical Shift References	124
4.3.3 Calibration of Transmitter Pulse Length	125
4.3.4 Calibration of Offset Frequencies	127
4.3.5 Calibration of Decoupler Pulse Length	130
4.3.6 Calibration of Decoupler Pulse Length with Off-Resonance Null	132
4.4 Selective Excitation with Narrow Band and Off-Resonance Shaped Pulses	133
4.5 Composite Pulses	136
4.5.1 Composite Excitation Pulses	136
4.5.2 Composite Pulses for Isotropic Mixing	136
4.5.3 Composite Pulses for Spin Decoupling	137
4.6 Adiabatic Pulses	139
4.7 Pulsed Field Gradients	141
4.8 Solvent Suppression	145
4.8.1 Presaturation	146
4.8.2 Watergate	147
4.8.3 Water Flip-Back	148
4.8.4 Jump-Return	149
4.9 NMR Data Processing	150
4.9.1 DC Drift Correction	150
4.9.2 Solvent Suppression Filter	150
4.9.3 Linear Prediction	151
4.9.4 Apodization	151
4.9.5 Zero Filling	154
4.9.6 Phase Correction	154
4.10 Two-Dimensional Experiments	158
4.10.1 The Second Dimension	158
4.10.2 Quadrature Detection in the Indirect Dimension	159
4.10.3 Selection of Coherence Transfer Pathways	161
4.10.4 COSY	163
4.10.5 DQF COSY	164
4.10.6 TOCSY	166
4.10.7 NOESY and ROESY	167
References	171

5	Multidimensional Heteronuclear NMR Experiments	173
5.1	Two-Dimensional Heteronuclear Experiments	173
5.1.1	HSQC and HMQC	174
5.1.2	HSQC Experiment Setup	176
5.1.3	Sensitivity-Enhanced HSQC by PEP	177
5.1.4	Setup of seHSQC Experiment	179
5.1.5	HMQC	180
5.1.6	IPAP HSQC	182
5.1.7	SQ-TROSY	184
5.2	Overview of Triple-Resonance Experiments	187
5.3	General Procedure of Setup and Data Processing for 3D Experiments	189
5.4	Experiments for Backbone Assignments	190
5.4.1	HNCO and HNCA	191
5.4.2	HN(CO)CA	198
5.4.3	HN(CA)CO	201
5.4.4	CBCANH	203
5.4.5	CBCA(CO)NH	206
5.5	Experiments for Side-Chain Assignment	209
5.5.1	HCCH-TOCSY	209
5.6	3D Isotope-Edited Experiments	214
5.6.1	¹⁵ N-HSQC-NOESY	214
5.7	Sequence-Specific Resonance Assignments of Proteins	216
5.7.1	Assignments Using ¹⁵ N-Labeled Proteins	216
5.7.2	Sequence-Specific Assignment Using Doubly Labeled Proteins	217
5.8	Assignment of NOE Cross Peaks	218
	References	219
6	Studies of Small Biological Molecules	223
6.1	Ligand-Protein Complexes	223
6.1.1	SAR-by-NMR Method	224
6.1.2	Diffusion Method	227
6.1.3	Transferred NOE	229
6.1.4	Saturation Transfer Difference	232
6.1.5	Isotope-Editing Spectroscopy	233
6.1.6	Isotope-Filtering Spectroscopy	235
6.2	Study of Metabolic Pathways by NMR	238
	References	244
7	Protein Structure Determination from NMR Data	247
7.1	Introduction and Historical Overview	247
7.2	NMR Structure Calculation Methods	249
7.2.1	Distance Geometry	250
7.2.2	Restrained Molecular Dynamics	251

7.3	NMR Parameters for Structure Calculation	253
7.3.1	Chemical Shifts	253
7.3.2	J Coupling Constants	254
7.3.3	Nuclear Overhauser Effect	255
7.3.4	Residual Dipolar Couplings	256
7.4	Preliminary Secondary Structural Analysis	258
7.5	Tertiary Structure Determination	259
7.5.1	Computational Strategies	259
7.5.2	Illustration of Step-by-Step Structure Calculations Using a Typical XPLOR Protocol	260
7.5.3	Criteria of Structural Quality	264
7.5.4	Second-Round Structure Calculation: Structure Refinement	265
7.5.5	Presentation of the NMR Structure	265
7.5.6	Precision of NMR Structures	266
7.5.7	Accuracy of NMR Structures	267
7.6	Protein Complexes	267
7.6.1	Protein–Protein Complexes	267
7.6.2	Protein–Peptide Complexes	268
Appendix B: sa.inp—Xplor Protocol for Protein Structure Calculation		269
Appendix C: Example of NOE Table		276
Appendix D: Example of Dihedral Angle Restraint Table		278
Appendix E: Example of Chemical Shift Table for Talos		281
Appendix F: Example of Hydrogen Bond Table		283
Appendix G: Example of Input File To Generate A Random-Coil Coordinates		284
Appendix H: Example of Input File to Generate a Geometric PSF File		285
References		286
8	Protein Dynamics	289
8.1	Theory of Spin Relaxation in Proteins	290
8.2	Experiments for Measurement of Relaxation Parameters	298
8.2.1	T ₁ Measurement	298
8.2.2	T ₂ and T _{1ρ} Measurements	302
8.2.3	Heteronuclear NOE Measurement	304
8.3	Relaxation Data Analysis	306
References		308
9	NMR-Based Metabolomics	311
9.1	Introduction	311
9.2	Fundamentals of Multivariate Statistical Analysis for Metabolomics	313

9.3	Sample Preparation	321
9.3.1	Phosphate Buffer for NMR Sample Preparation	321
9.3.2	Urine Samples	322
9.3.3	Blood Plasma and Serum	323
9.3.4	Tissue Sample Quench, Storage, and Extraction	324
9.3.5	Culture Adherent Cells	326
9.3.6	Quench and Extract Cells	328
9.4	Practical Aspects of NMR Experiments	332
9.4.1	Calibration	332
9.4.2	Automation	332
9.4.3	NMR Experiments	336
9.5	Data Analysis and Model Interpretation	343
9.5.1	NMR Data Processing and Normalization	344
9.5.2	Analysis of Metabolomic Data	351
9.6	Metabolomics of Biofluids	361
9.7	Cellular Metabolomics	370
9.7.1	Experiments	370
9.7.2	NMR Data Processing	373
9.7.3	Principal Component Analysis	373
9.7.4	Partial Least Squares for Discriminant Analysis	376
9.8	Metabolomics of Live Cell	377
9.9	Metabolomics Applied to Cancer Research	382
9.9.1	Silibinin Anticancer Efficacy	383
9.9.2	Metabolomic Profiling of Colon Cancer	385
	References	388
	Appendix I: Multiple Choice Questions	393
	Appendix J: Nomenclature and Symbols	413
	Index	417

Chapter 1

Basic Principles of NMR

1.1 Introduction

Energy states and population distribution are the fundamental subjects of any spectroscopic technique. The energy difference between energy states gives rise to the frequency of the spectra, whereas intensities of the spectral peaks are proportional to the population difference of the states. Relaxation is another fundamental phenomenon in nuclear magnetic resonance spectroscopy (NMR), which influences both line shapes and intensities of NMR signals. It provides information about structure and dynamics of molecules. Hence, understanding these aspects lays the foundation to understanding basic principles of NMR spectroscopy.

In principle, an NMR spectrometer is more or less like a radio. In a radio, audio signals in the frequency range of kilohertz are the signals of interest, which one can hear. However, the signals sent by broadcast stations are in the range of 100 MHz for FM and of up to 1 GHz for AM broadcasting. The kilohertz audio signals must be separated from the megahertz transmission frequencies before they are sent to speakers. In NMR spectroscopy, nuclei have an intrinsic megahertz frequency which is known as the Larmor frequency. For instance, in a molecule, all protons have the same Larmor frequency. However, the signals of interest are the chemical shifts generated by the electron density surrounding an individual proton, which are in the kilohertz frequency range. Many of the protons in the molecule have different chemical environments which give different signals in the kilohertz range. One must find a way to eliminate the megahertz Larmor frequency in order to observe the kilohertz chemical shifts (more details to follow).

1.2 Nuclear Spin in a Static Magnetic Field

1.2.1 Precession of Nuclear Spins in a Magnetic Field

As mentioned above, energy and population associated with energy states are the bases of the frequency position and the intensity of spectral signals. In order to understand the principles of NMR spectroscopy, it is necessary to know how the energy states of nuclei are generated and what are the energy and population associated with the energy states.

Key questions to be addressed in this section include the following:

1. What causes nuclei to precess in the presence of magnetic field?
2. What kind of nuclei will give NMR signals?
3. How do nuclear spins orient in the magnetic field?

Not any kind of nucleus will give NMR signals. Nuclei with an even number of both charge and mass have a spin quantum number of zero, e.g., ^{12}C . These kinds of nuclei do not have nuclear angular momentum and will not give rise to NMR signal; these are called NMR inactive nuclei. For nuclei with nonzero spin quantum number, energy states are produced by the nuclear angular momentum interacting with the applied magnetic field. Nuclei with nonzero spin quantum number possess nuclear angular momentum whose magnitude is determined by:

$$P = \hbar\sqrt{I(I+1)} \quad (1.1)$$

in which I is the nuclear spin quantum number and \hbar is the Planck constant divided by 2π . The value of I is dependent on the mass and charge of nucleus, and it can be either an integral or half integral number. The z component of the angular momentum is given by:

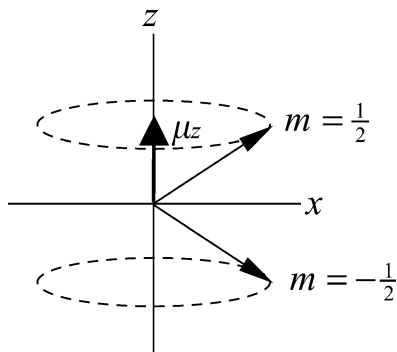
$$P_z = \hbar m \quad (1.2)$$

in which the magnetic quantum number m has possible values of $I, I-1, \dots, -I+1, -I$, and a total of $2I+1$. This equation tells us that the projection of nuclear angular momentum on the z axis is quantized in space and has a total of $2I+1$ possible values. The orientations of nuclear angular momentum are defined by the allowed m values. For example, for spin $\frac{1}{2}$ nuclei, the allowed m are $\frac{1}{2}$ and $-\frac{1}{2}$. Thus, the angular momentum of spin $\frac{1}{2}$ ($I=\frac{1}{2}$) has two orientations, one is pointing up (pointing to z axis) and the other pointing down (pointing to $-z$ axis) with an angle of 54.7° relative to the magnetic field (Fig. 1.1).

The nuclei with a nonzero spin quantum number will rotate about the magnetic field B_0 due to the torque generated by the interaction of the nuclear angular momentum with the magnetic field. The magnetic moment (or nuclear moment), μ , is either parallel or antiparallel to their angular momentum:

$$\mu = \gamma P = \gamma\hbar\sqrt{I(I+1)} \quad (1.3)$$

Fig. 1.1 Orientation of nuclear angular momentum μ with spin $\frac{1}{2}$ and its z component, μ_z . The vectors represent the angular momentum μ rotating about the magnetic field whose direction is along the z axis of the laboratory frame



in which γ is the nuclear gyromagnetic ratio, which has a specific value for a given isotope. Thus, γ is a characteristic constant for a specific nucleus. The angular momentum P is the same for all nuclei with the same magnetic quantum number, whereas the angular momentum μ is different for different nuclei. For instance, ^{13}C and ^1H have same angular momentum P because they have same spin quantum number of $\frac{1}{2}$, but have different angular moments μ because they are different isotopes with different γ . Therefore, nuclear angular momentum μ is used to characterize nuclear spins. The moment μ is parallel to angular momentum if γ is positive or antiparallel if γ is negative (e.g., ^{15}N). Similar to the z component of angular momentum, P_z , the z component of angular momentum μ_z is given by:

$$\mu_z = \gamma P_z = \gamma \hbar m \quad (1.4)$$

The equation indicates that μ_z has a different value for different nuclei even if they may have same magnetic quantum number m . When nuclei with a nonzero spin quantum number are placed in a magnetic field, they will precess about the magnetic field due to the torque generated by the interaction of the magnetic field B_0 with the nuclear moment μ . The angle of μ relative to B_0 is dependent on m . Nuclei with nonzero spin quantum numbers are also called nuclear spins because their angular moments make them spin in the magnetic field.

In summary, the nuclear angular momentum is what causes the nucleus to rotate relative to the magnetic field. Different nuclei have a characteristic nuclear moment because the moment is dependent on the gyromagnetic ratio γ , whereas nuclei with the same spin quantum number possess the same nuclear angular momentum. Nuclear moments have quantized orientations defined by the value of the magnetic quantum number, m . The interaction of nuclei with the magnetic field is utilized to generate an NMR signal. Because the energy and population of nuclei are proportional to the magnetic field strength (more details discussed below), the frequency and intensity of the NMR spectral signals are dependent on the field strength.

1.2.2 Energy States and Population

It has been illustrated in the previous section that nuclei with nonzero spin quantum numbers orient along specific directions with respect to the magnetic field. They are rotating continuously about the field direction due to the nuclear moment μ possessed by nuclei. For each orientation state, also known as the Zeeman state or spin state, there is energy associated with it, which is characterized by the frequency of the precession.

Key questions to be addressed in this section include the following:

1. What is the energy and population distribution of the Zeeman states?
2. What are the nuclear precession frequencies of the Zeeman states and the frequency of the transition between the states, and how are they different?
3. How are energy and population related to the measurable spectral quantities?

The intrinsic frequency of the precession is the Larmor frequency ω_0 . The energy of the Zeeman state with magnetic quantum number m can be described in terms of the Larmor frequency:

$$E = -\mu_z B_0 = -m\hbar\gamma B_0 = m\hbar\omega_0 \quad (1.5)$$

in which B_0 is the magnetic field strength in the unit of tesla, T, and $\omega_0 = -\gamma B_0$ is the Larmor frequency. Therefore, the energy difference in the allowed transition (the selection rule is that only single-quantum transition, i.e., $\Delta m = \pm 1$, is allowed), for instance, between the $m = -\frac{1}{2}$ and $m = \frac{1}{2}$ Zeeman states is given by:

$$\Delta E = \hbar\gamma B_0 \quad (1.6)$$

Because $\Delta E = \hbar\omega$, the frequency of the required electromagnetic radiation for the transition has the form of:

$$\omega_0 = \gamma B_0 \quad (1.7)$$

which has a linear dependence on the magnetic field strength. Commonly, the magnetic field strength is described by the proton Larmor frequency at the specific field strength. A proton resonance frequency of 100 MHz is corresponding to the field strength of 2.35 T. For example, a 600 MHz magnet has a field strength of 14.1 T. While the angular frequency ω has a unit of radian per second, the frequency can also be represented in hertz with the relationship of:

$$\nu = \frac{\omega}{2\pi} \quad (1.8)$$

As the magnetic field strength increases, the energy difference between two transition states becomes larger, as does the frequency associated with the Zeeman transition. The intensity of the NMR signal comes from the population difference of

two Zeeman states of the transition. The population of the energy state is governed by the Boltzmann distribution. For a spin $1/2$ nucleus with a positive γ such as ^1H , or ^{13}C , the lower energy state (ground state) is defined as the α state for $m = 1/2$, whereas the higher energy state (excited state) is labeled as the β state for $m = -1/2$. For ^{15}N , $m = -1/2$ is the lower energy α state because of its negative γ . The ratio of the populations in the states is quantitatively described by the Boltzmann equation:

$$\frac{N_\beta}{N_\alpha} = e^{-\Delta E/kT} = e^{-\hbar\gamma B_0/kT} = \frac{1}{e^{\hbar\gamma B_0/kT}} \quad (1.9)$$

in which N_α and N_β are the population of α and β states, respectively, T is the temperature in Kelvin and k is the Boltzmann constant. The equation states that both the energy difference of the transition states and the population difference of the states increases with the magnetic field strength. Furthermore, the population difference has a temperature dependence. If the sample temperature reaches the absolute zero, there is no population at β state and all spins will lie in α state, whereas both states will have equal population if the temperature is infinitely high. At T near room temperature, ~ 300 K, $\hbar\gamma B_0 \ll kT$. As a consequence, a first-order Taylor expansion can be used to describe the population difference:

$$\frac{N_\beta}{N_\alpha} \approx 1 - \frac{\hbar\gamma B_0}{kT} \quad (1.10)$$

At room temperature, the population of the β state is slightly lower than that of the α state. For instance, the population ratio for protons at 800 MHz is 0.99987. This indicates that only a small fraction of the spins will contribute to the signal intensity due to the low energy difference and hence NMR spectroscopy intrinsically is a very insensitive spectroscopic technique. Therefore, a higher magnetic field is necessary to obtain better sensitivity, in addition to other advantages such as resolution and the TROSY effect (transverse relaxation optimized spectroscopy).

1.2.3 Bulk Magnetization

Questions to be addressed in this section include the following:

1. What is the bulk magnetization and where is it located?
2. Why do no transverse components of the bulk magnetization exist at the equilibrium?

The observable NMR signals come from the assembly of the nuclear spins in the presence of the magnetic field. It is the bulk magnetization of a sample (or macroscopic magnetization) that gives the observable magnetization, which is the vector sum of all spin moments (nuclear angular moments). Because nuclear

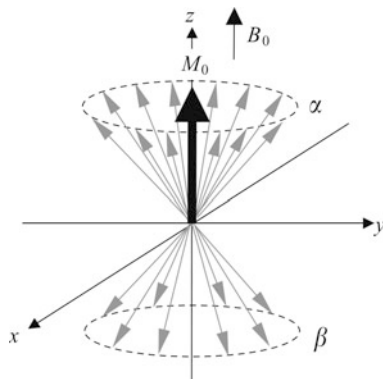


Fig. 1.2 Bulk magnetization of spin $\frac{1}{2}$ nuclei with positive γ . x , y , and z are the axes of the laboratory frame. The *thin arrows* represent individual nuclear moments. The vector sum of the nuclear moments on the xy plane is zero because an individual nuclear moment has equal probability of being in any direction of the xy plane. The bulk magnetization M_0 , labeled as a *thick arrow*, is generated by the small population difference between the α and β states, and is parallel to the direction of the static magnetic field B_0

spins precess about the magnetic field along the z axis of the laboratory frame, an individual nuclear moment has equal probability of being in any direction of the xy plane. Accordingly, the transverse component of the bulk magnetization at the equilibrium state is averaged to zero and hence is not observable (Fig. 1.2). The bulk magnetization M_0 results from the small population difference between the α and β states. At equilibrium, this vector lies along the z axis and is parallel to the magnetic field direction for nuclei with positive γ because the spin population in the α state is larger than that in the β state. Although the bulk magnetization is stationary along the z axis, the individual spin moments rotate about the axis.

1.3 Rotating Frame

Question to be addressed in this section include the following:

1. What is the rotating frame and why is it needed?
2. What is the B_1 field and why must it be an oscillating electromagnetic field?
3. How does the bulk magnetization M_0 react when a B_1 field is applied to it?
4. What is the relationship between radio frequency (RF) pulse power and pulse length?

The Larmor frequency of a nuclear isotope is the resonance frequency of the isotope in the magnetic field. For example, ^1H Larmor frequency will be 600 MHz for all protons of a sample in the magnetic field of 14.1 T. If the Larmor frequency were the only observed NMR signal, NMR spectroscopy would not be useful because there would be only one resonance signal for all ^1H . In fact, chemical shifts are the NMR signals of interest (details in Sect. 1.7), which have a frequency range

of kilohertz, whereas the Larmor frequency of all nuclei is in the range of megahertz. For instance, the observed signals of protons are normally in the range of several kilohertz with a Larmor frequency of 600 MHz in the magnetic field of 14.1 T. How the Larmor frequency is removed before NMR data are acquired, what the rotating frame is, why we need it and how the bulk magnetization changes upon applying an additional electromagnetic field are the topics of this section.

Since the Larmor frequency will not be present in any NMR spectrum, it is necessary to remove its effect when dealing with signals in frequency range of kilohertz. This can be done by applying an electromagnetic field B_1 along an axis on the xy plane of the laboratory frame, which rotates at the Larmor frequency with respect to the z axis of the laboratory frame. This magnetic field is used for the purposes of (a) removing the effect of the Larmor frequency and hence simplifying the theoretical and practical consideration of the spin precession in NMR experiments, and (b) inducing the nuclear transition between two energy states by its interaction with the nuclei in the sample according to the resonance condition that the transition occurs when the frequency of the field equals the resonance frequencies of the nuclei. This magnetic field is turned on only when it is needed. Because the Larmor frequency is not observed in NMR experiments, a new coordinate frame is introduced to eliminate the Larmor frequency from consideration, called the rotating frame. In the rotating frame, the xy plane of the laboratory frame is rotating at or near the Larmor frequency ω_0 with respect to the z axis of the laboratory frame. The transformation of the laboratory frame to the rotating frame can be illustrated by taking a carousel (also known as merry-go-round) as an example. The carousel observed by one standing on the ground is rotating at a given speed. When one is riding on it, he is also rotating at the same speed. However, he is stationary relative to others on the carousel. If the ground is considered the laboratory frame, the carousel is the rotating frame. When the person on the ground steps onto the carousel, it is the transformation from the laboratory frame to the rotating frame. The sole difference between the laboratory frame and the rotating frame is that the rotating frame is rotating in the xy plane about the z axis relative to the laboratory frame.

By transforming from the laboratory frame to the rotating frame, the nuclear moments are no longer spinning about the z axis, i.e., they are stationary in the rotating frame. The term “transforming” here means that everything in the laboratory frame will rotate at a frequency of $-\omega_0$ about the z axis in the rotating frame. As a result, the bulk magnetization does not have its Larmor frequency in the rotating frame. Since the applied B_1 field is rotating at the Larmor frequency in the laboratory frame, the transformation of this magnetic field to the rotating frame results in a stationary B_1 field along an axis on the xy plane in the rotating frame, for example the x axis. Therefore, when this B_1 magnetic field is applied, its net effect on the bulk magnetization is to rotate the bulk magnetization away from the z axis clockwise about the axis of the applied field by the left-hand rule in the vector representation.

In practice, the rotation of the B_1 field with respect to the z axis of the laboratory frame is achieved by generating a linear oscillating electromagnetic field with the magnitude of $2B_1$ because it is easily produced by applying electric current through

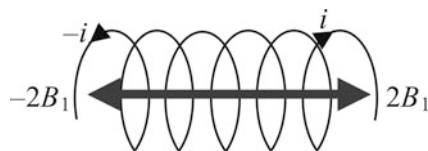


Fig. 1.3 The electromagnetic field generated by the current passing through the probe coil. The magnitude of the field is modulated by changing the current between $-i$ and $+i$. The electromagnetic field is called the oscillating B_1 field

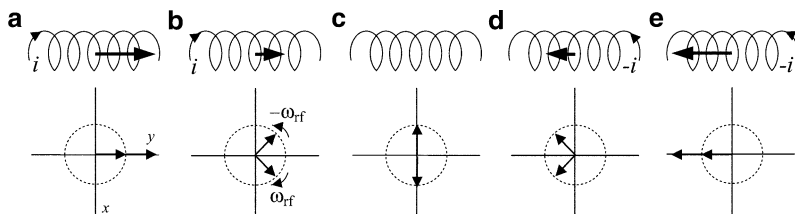
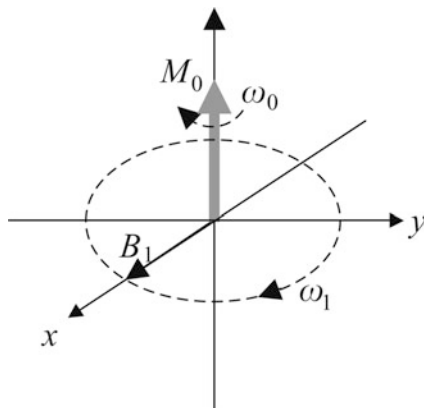


Fig. 1.4 Vector sum of the oscillating B_1 field generated by passing current through a probe coil. The magnitude of the field can be represented by two equal amplitude vectors rotating in opposite directions. The angular frequency of the two vectors is the same as the oscillating frequency ω_{rf} of the B_1 field. When $\omega_{rf} = \omega_0$, B_1 is said to be on resonance. (a) When the current reaches the maximum, the two vectors align on y axis. The sum of the two vectors is the same as the field produced in the coil. (b) As the B_1 field reduces, its magnitude equals the sum of the projections of two vectors on the y axis. (c) When the two vectors are oppositely aligned on the x axis, the current in the coil is zero. (d) As the current reduces, both components rotate into the $-y$ region and the sum produces a negative magnitude. (e) Finally, the two components meet at the $-y$ axis, which represents a field magnitude of $-2B_1$. At any given time the two decomposed components have the same magnitude of B_1 , the same frequency of ω_{rf} and are mirror image to each other

the probe coil (Fig. 1.3). The oscillating magnetic field has a frequency equal to the Larmor frequency of the nuclei. As the current increases from zero to maximum, the field proportionally increases from zero to the maximum field along the coil axis ($2B_1$ in Fig. 1.3). Reducing the current from the maximum to zero and then to the minimum (negative maximum, $-i$) decreases the field from $2B_1$ to $-2B_1$. Finally, the field is back to zero from $-2B_1$ as the current is increased from the minimum to zero to finish one cycle. If the frequency of changing the current is ν_{rf} , we can describe the oscillating frequency as ω_{rf} ($\omega = 2\pi\nu$). Mathematically, this linear oscillating field (thick arrow in Fig. 1.4) can be represented by two equal fields with half of the magnitude, B_1 , rotating in the xy plane at the same angular frequency in opposite directions to each other (thin arrows). When the field has the maximum strength at $2B_1$, each component aligns on the y axis with a magnitude of B_1 . The vector sum of the two is $2B_1$ (Fig. 1.4a). When the current is zero, which gives zero in the field magnitude, each component still has the same magnitude of B_1 but aligns on the x and $-x$ axes, respectively, which gives rise to a vector sum of zero (Fig. 1.4c). As the current reduces, both components rotate into

Fig. 1.5 B_1 field in the laboratory frame. The bulk magnetization M_0 is the vector sum of individual nuclear moments which are precessing about the static magnetic field B_0 at the Larmor frequency ω_0 . When the angular frequency ω_{rf} of the B_1 field is equal to the Larmor frequency, that is, $\omega_{\text{rf}} = \omega_0$, the B_1 field is on resonance



the $-y$ region and the sum produces a negative magnitude (Fig. 1.4d). Finally, the two components meet at the $-y$ axis, which represents a field magnitude of $-2B_1$ (Fig. 1.4e). At any given time the two decomposed components have the same magnitude of B_1 , the same frequency of ω_{rf} and are mirror image to each other.

If the frequency of the rotating frame is set to ω_{rf} which is close to the Larmor frequency ω_0 , the component of the B_1 field which has ω_{rf} in the laboratory frame has null frequency in the rotating frame because of the transformation by the $-\omega_{\text{rf}}$. The other with $-\omega_{\text{rf}}$ in the laboratory frame now has an angular frequency of $-2\omega_{\text{rf}}$ after the transformation. Since the latter has a frequency far away from the Larmor frequency it will not interfere with the NMR signals which are in the range of kilohertz. Therefore, this component is ignored throughout the discussion unless specifically mentioned. The former component with null frequency in the rotating frame is used to represent the B_1 field. If we regulate the frequency of the current oscillating into the coil as ω_0 , then setting ω_{rf} to equal the Larmor frequency ω_0 , the B_1 field is said to be on resonance (Fig. 1.5). Since in the rotating frame the Larmor frequency is not present in the nuclei, the effect of B_0 on nuclear spins is eliminated. The only field under consideration is the B_1 field. From the earlier discussion we know that nuclear magnetization will rotate about the applied field direction upon its interaction with a magnetic field. Hence, whenever B_1 is turned on, the bulk magnetization will be rotated about the axis where B_1 is applied in the rotating frame. The frequency of the rotation is determined by:

$$\omega_1 = \gamma B_1 \quad (1.11)$$

This should not be misunderstood as ω_{rf} of the B_1 field since ω_{rf} is the field oscillating frequency determined by changing the direction of the current passing through the coil, which is set to be the same as or near the Larmor frequency. The frequency ω_{rf} is often called the carrier frequency or the transmitter frequency. The frequency ω_1 is determined by the amplitude of the B_1 field, i.e., the maximum strength of the B_1 field. By modulating the amplitude and time during which B_1

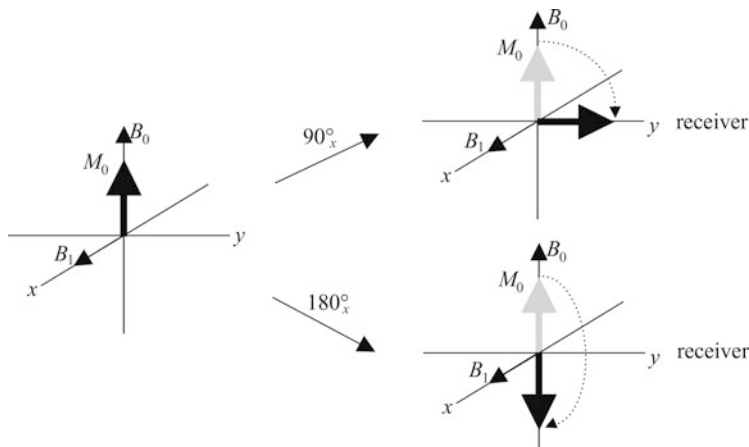


Fig. 1.6 Vector representation of the bulk magnetization upon applying a 90° pulse and a 180° pulse by the B_1 along the x axis in the rotating frame. The maximum signal is obtained when a 90° pulse is applied, which rotates the bulk magnetization (M_0) onto the xy plane. No signal is observed when a 180° pulse is applied, which rotates M_0 to $-z$ axis

is turned on, the bulk magnetization can be rotated to anywhere in the plane perpendicular to the axis of the applied B_1 field in the rotating frame. If B_1 is turned on, and then turned off when M_0 moves from the z axis to the xy plane, this is called a 90° pulse. The corresponding time during which B_1 is applied is called the 90° pulse length (or the 90° pulse width), and the field amplitude is called the pulse power. A 90° pulse length can be as short as a few microseconds and as long as a fraction of a second. The pulse power for a hard (short) 90° pulse is usually as high as half of a hundred watts for proton and several hundred watts for heteronuclei (all nuclei except ^1H). Because heteronuclei have lower gyromagnetic ratios than proton, they have longer 90° pulse lengths at a given B_1 field strength.

The 90° pulse length (pw_{90}) is proportional to the B_1 field strength:

$$v_1 = \frac{\gamma B_1}{2\pi} = \frac{1}{4\text{pw}_{90}} \quad (1.12)$$

$$\text{pw}_{90} = \frac{\pi}{2\gamma B_1} = \frac{1}{4v_1} \quad (1.13)$$

in which v_1 is the field strength in the frequency unit of hertz. A higher B_1 field produces a shorter 90° pulse. A 90° pulse of $10 \mu\text{s}$ is corresponding to a 25 kHz B_1 field. Nuclei with smaller gyromagnetic ratios will require a higher B_1 to generate the same pw_{90} as that with larger γ . When a receiver is placed on the transverse plane of the rotating frame, NMR signals are observed from the transverse magnetization. The maximum signal is obtained when the bulk magnetization is in the xy plane of the rotating frame, which is done by applying a 90° pulse. No signal is observed when a 180° pulse is applied (Fig. 1.6).

1.4 Bloch Equations

As we now know, the nuclei inside the magnet produce nuclear moments which cause them to spin about the magnetic field. In addition, the interaction of the nuclei with the magnetic field will rotate the magnetization towards the transverse plane when the electromagnetic B_1 field is applied along a transverse axis in the rotating frame. After the pulse is turned off, the magnetization is solely under the effect of the B_0 field. How the magnetization changes with time can be described by the Bloch equations, which are based on a simple vector model.

Questions to be addressed in the current section include the following:

1. What phenomena do the Bloch equations describe?
2. What is free induction decay?
3. What are limitations of the Bloch equations?

In the presence of the magnetic field B_0 , the torque produced by B_0 on spins with the angular moment μ causes precession of the nuclear spins. Felix Bloch derived simple semiclassical equations to describe the time-dependent phenomena of nuclear spins in the static magnetic field (Bloch 1946). The torque on the bulk magnetization, described by the change of the angular momentum as a function of time, is given by:

$$T = \frac{dP}{dt} = M \times B \quad (1.14)$$

in which $M \times B$ is the vector product of the bulk magnetization M (the sum of μ) with the magnetic field B . Because $M = \gamma P$ (or $P = M/\gamma$) according to (1.3), the change of magnetization with time is described by:

$$\frac{dM}{dt} = \gamma(M \times B) \quad (1.15)$$

When B is the static magnetic field B_0 which is along the z axis of the laboratory frame, the change of magnetization along the x , y , and z axes with time can be obtained from the determinant of the vector product:

$$\frac{dM}{dt} = i \frac{dM_x}{dt} + j \frac{dM_y}{dt} + k \frac{dM_z}{dt} = \gamma \begin{vmatrix} i & j & k \\ M_x & M_y & M_z \\ 0 & 0 & B_0 \end{vmatrix} = i\gamma M_y B_0 - j\gamma M_x B_0 \quad (1.16)$$

in which i, j, k are the unit vectors along the x, y , and z axes, respectively. Therefore,

$$\frac{dM_x}{dt} = \gamma M_y B_0 \quad (1.17)$$

$$\frac{dM_y}{dt} = -\gamma M_x B_0 \quad (1.18)$$

$$\frac{dM_z}{dt} = 0 \quad (1.19)$$

The above Bloch equations describe the time dependence of the magnetization components under the effect of the static magnetic field B_0 produced by the magnet of an NMR spectrometer without considering any relaxation effects. The z component of the bulk magnetization M_z is independent of time, whereas the x and y components are decaying as a function of time and the rate of the decay is dependent on the field strength and nuclear gyromagnetic ratio. The Bloch equations can be represented in the rotating frame, which is related to their form in the laboratory frame according to the following relationship:

$$\left(\frac{dM}{dt}\right)_{\text{rot}} = \left(\frac{dM}{dt}\right)_{\text{lab}} + M \times \omega = M \times (\gamma B + \omega) = M \times \gamma B_{\text{eff}} \quad (1.20)$$

in which $B_{\text{eff}} = B + \omega/\gamma$ and ω is the angular frequency of the rotating frame and is the same as ω_{rf} . The motion of magnetization in the rotating frame is the same as in the laboratory frame, provided the field B is replaced by the effective field B_{eff} . When $\omega = -\gamma B = \omega_0$, the effective field disappears, resulting in time-independent magnetization in the rotating frame. It is worth noting that $-\gamma B$ is the Larmor frequency of the magnetization according to (1.5), whereas γB is the transformation from the laboratory frame to the rotating frame, $-\omega_{\text{rf}}$ (Sect. 1.3).

Since the bulk magnetization at equilibrium is independent of time, based on the Bloch equations it is not an observable NMR signal. The observable NMR signals are the time-dependent transverse magnetization. However, at equilibrium the net xy projections of the magnetization (nuclear angular moments) are zero due to the precession of the nuclear spins. The simple solution to this is to bring the bulk magnetization to the xy plane by applying the B_1 electromagnetic field. The transverse magnetization generated by the B_1 field (90° pulse) will not stay in the transverse plane indefinitely; instead it decays under the interaction of the static magnetic field B_0 while precessing about the z axis and realigns along the magnetic field direction or the z axis of the laboratory frame (Fig. 1.7). The decay of the transverse magnetization forms the observable NMR signals detected by the receiver in the xy plane in the rotating frame, which is called the free induction decay, or FID.

The Bloch theory has its limitations in describing spin systems with nuclear interactions other than chemical shift interaction, such as strong scalar coupling. In general, the Bloch equations are applied to systems of noninteracting spin $1/2$ nuclei. Nevertheless, it remains a very useful tool to illustrate simple NMR experiments.

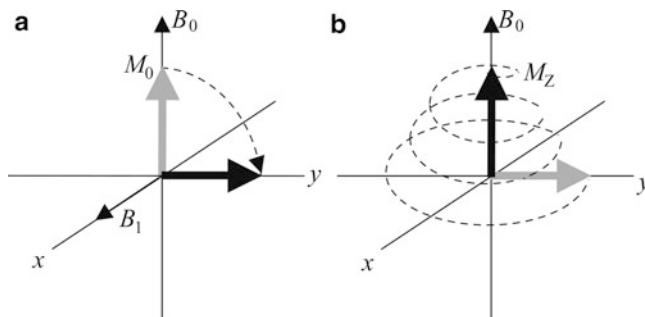


Fig. 1.7 Vector model representation of a one-pulse experiment. (a) The equilibrium bulk magnetization shown in the *shaded arrow* is brought to *y* axis by a 90° pulse along the *x* axis. (b) After the 90° pulse, the transverse magnetization decays back to the initial state while precessing about the *z* axis. An FID is observed by quadrature detection on the transverse plane

1.5 Fourier Transformation and Its Applications in NMR

The free induction decay is the sum of many time domain signals with different frequencies, amplitudes and phases. These time domain signals are detected and digitized during the signal acquisition period. In order to separate the individual signals and display them in terms of their frequencies (spectrum), the time domain data (FID) are converted to a frequency spectrum by applying the Fourier transformation, named after the discovery by French mathematician Joseph Fourier.

Question to be addressed in this section include the following:

1. What are the properties of the Fourier transformation useful for NMR?
2. What is the relationship between excitation bandwidth and pulse length in terms of the Fourier transformation?
3. What is quadrature detection and why is it necessary?

1.5.1 Fourier Transformation and Its Properties Useful for NMR

The Fourier transformation describes the connection between two functions with dependent variables such as time and frequency ($\omega = 2\pi/t$), called a Fourier pair, by the relationship (Bracewell 1986):

$$F(\omega) = \text{Ft}\{f(t)\} = \int_{-\infty}^{\infty} f(t)e^{-i\omega t} dt \quad (1.21)$$

$$f(t) = \text{Ft}\{F(\omega)\} = \frac{1}{2\pi} \int_{-\infty}^{\infty} F(\omega)e^{i\omega t} d\omega \quad (1.22)$$

Although there are many methods to perform the Fourier transformation for the NMR data, the Cooley–Tukey fast FT algorithm is commonly used to obtain NMR spectra from FIDs combined with techniques such as maximum entropy (Sibisi et al. 1984; Mazzeo et al. 1989; Stern and Hoch 1992) and linear prediction (Zhu and Bax 1990; Barkhausen et al. 1985). For NMR signals described as an exponential function (or sine and cosine pair) with a decay constant $1/T$, the Fourier pair is the FID and spectrum with the forms of:

$$f(t) = e^{(i\omega_0 - (1/T))t} \quad (1.23)$$

$$F(\omega) = \text{Ft}\{f(t)\} = \int_{-\infty}^{\infty} e^{(i\omega_0 - (1/T))t} e^{-i\omega t} dt = \frac{i(\omega_0 - \omega) + (1/T)}{(\omega_0 - \omega)^2 + (1/T^2)} \quad (1.24)$$

which indicate that the spectrum is obtained by the Fourier transformation of the FID and the frequency signal has a Lorentzian line shape. Some important properties of the Fourier transformation useful in NMR spectroscopy are discussed below (Harris and Stocker 1998):

1. *Linearity theorem.* The Fourier transform of the sum of functions is the same as the sum of Fourier transforms of the functions:

$$\text{Ft}\{f(t) + g(t)\} = \text{Ft}\{f(t)\} + \text{Ft}\{g(t)\} \quad (1.25)$$

This tells us that the sum of time domain data such as an FID will yield individual frequency signals after the Fourier transformation.

2. *Translation theorem.* The Fourier transform of a function shifted by time τ is equal to the product of the Fourier transform of the unshifted function by a factor of $e^{i\omega\tau}$:

$$\text{Ft}\{f(t + \tau)\} = e^{i\omega\tau} \text{Ft}\{f(t)\} = e^{i2\pi\phi} \text{Ft}\{f(t)\} \quad (1.26)$$

This states that a delay in the time function introduces a frequency-dependent phase shift in the frequency function. A delay in the acquisition of the FID will cause a first-order phase shift (frequency-dependent phase shift) in the corresponding spectrum. This also allows the phase of a spectrum to be adjusted after acquisition without altering the signal information contained in the time domain data $f(t)$ (FID). The magnitude representation of the spectrum is unchanged by spectral phasing because the integration of $|\exp(i\omega t)|$ over all possible ω yields unity. Similarly,

$$\text{Ft}\{f(\omega - \omega_0)\} = e^{i\omega_0\tau} f(t) \quad (1.27)$$

A frequency shift in a spectrum is equivalent to an oscillation in the time domain with the same frequency. This allows the spectral frequency to be calibrated after acquisition.

3. *Convolution theorem.* The Fourier transform of the convolution of functions f_1 and f_2 is equal to the product of the Fourier transforms of f_1 and f_2 :

$$\text{Ft}\{f_1(t) * f_2(t)\} = \text{Ft}[f_1(t)] * \text{Ft}[f_2(t)] \quad (1.28)$$

in which the convolution of two functions is defined as the time integral over the product of one function and the other shifted function:

$$f_1(t) * f_2(t) = \int_{-\infty}^{\infty} f_1(\tau)f_2(t - \tau) d\tau \quad (1.29)$$

Based on this theorem, desirable line shapes of frequency signals can be obtained simply by applying a time function to the acquired FID prior to the Fourier transformation to change the line shape of the spectral peaks, known as apodization of the FID (see Sect. 4.9.4).

4. *Scaling theorem.* The Fourier transform of a function with which a scaling transformation is carried out ($t \rightarrow t/c$) is equal to the Fourier transform of the original function with the transformation $\omega \rightarrow c\omega$ multiplied by the absolute value of factor c :

$$\text{Ft}\{f(t/c)\} = |c|F(c\omega) \quad (1.30)$$

According to this theorem, the narrowing of the time domain function by a factor of c causes the broadening of its Fourier transformed function in frequency domain by the same factor, and vice versa. This theorem is also known as similarity theorem.

5. *Parseval's theorem.*

$$\int_{-\infty}^{\infty} |f(t)|^2 dt = \int_{-\infty}^{\infty} |F(v)|^2 dv = \int_{-\infty}^{\infty} |F(\omega)|^2 d\omega \quad (1.31)$$

This theorem indicates that the information possessed by the signals in both time domain and frequency domain is identical.

1.5.2 Excitation Bandwidth

In order to excite the transitions covering all possible frequencies, the excitation bandwidth is required to be sufficiently large. This requirement is achieved by applying short RF pulses. In certain other situations, the excitation bandwidth is

required to be considerably narrow to excite a narrow range of resonance frequency such as in selective excitation. The following relationships of Fourier transformation pairs are helpful in understanding the process.

A Dirac delta function $\delta(t - \tau)$ in the time domain at $t = \tau$ gives rise to a spectrum with an infinitely wide frequency range and uniform intensity:

$$\text{Ft}\{\delta(t - \tau)\} = \int_{-\infty}^{\infty} \delta(t - \tau)e^{-i\omega t} dt = e^{-i\omega\tau} \quad (1.32)$$

which produces a frequency domain function with a perfectly flat magnitude at all frequencies because $|e^{-i\omega\tau}| = 1$. The δ function can be considered as an infinitely short pulse centered at τ . This infinitely short pulse excites an infinitely wide frequency range. When τ equals zero, each frequency has the same phase. Equation (1.32) means that in order to excite a wide frequency range, the RF pulse must be sufficiently short. Alternatively, for selective excitation, a narrow range of frequency is excited when a long RF pulse is used. A δ function in the frequency domain representing a resonance at frequency ω_0 with a unit magnitude has a flat constant magnitude in the time domain lasting infinitely long in time:

$$\text{Ft}\{e^{i\omega_0 t}\} = \int_{-\infty}^{\infty} e^{i\omega_0 t} e^{-i\omega t} dt = 2\pi\delta(\omega - \omega_0) \quad (1.33)$$

For a single resonance excitation, the RF pulse is required to be infinitely long. In practice, the short pulses are a few microseconds, which are usually called hard pulses, whereas the long pulses may last a few seconds, and are called selective pulses. Shown in Fig. 1.8 are the Fourier transforms of the short and long pulses. The bandwidth of the short pulse may cover several kilohertz and the selectivity of a long pulse can be as narrow as several hertz. A Gaussian function is the only function whose Fourier transformation gives another same-type (Gaussian) function (Fig. 1.8d, h):

$$\text{Ft}\{e^{-(t^2/\sigma^2)}\} = \int_{-\infty}^{\infty} e^{-(t^2/\sigma^2)} e^{-i\omega t} dt = -\sigma\sqrt{\pi}e^{-(\omega^2\sigma^2/4)} \quad (1.34)$$

A Gaussian shaped pulse will selectively excite a narrow range of frequency. The value of σ determines the selectivity of the pulse. The broadening of a Gaussian pulse results in narrowing in the frequency domain. More details on selective shaped pulses are discussed in Chap. 4.